



Data Reproducibility of Spin-Echo Small-Angle Neutron Scattering Instruments

Fumiaki Funama, Gregory N. Smith, Steven R. Parnell, Chris P. Duif, Wim G. Bouwman, Roger Pynn, Robert M. Dalgliesh & Fankang Li

To cite this article: Fumiaki Funama, Gregory N. Smith, Steven R. Parnell, Chris P. Duif, Wim G. Bouwman, Roger Pynn, Robert M. Dalgliesh & Fankang Li (11 Mar 2025): Data Reproducibility of Spin-Echo Small-Angle Neutron Scattering Instruments, Neutron News, DOI: [10.1080/10448632.2025.2468088](https://doi.org/10.1080/10448632.2025.2468088)

To link to this article: <https://doi.org/10.1080/10448632.2025.2468088>



© 2025 The Author(s). Published with license by Taylor & Francis Group, LLC



View supplementary material [↗](#)



Published online: 11 Mar 2025.



Submit your article to this journal [↗](#)



View related articles [↗](#)



View Crossmark data [↗](#)

Data Reproducibility of Spin-Echo Small-Angle Neutron Scattering Instruments

FUMIAKI FUNAMA¹ , GREGORY N. SMITH² , STEVEN R. PARNELL^{2,3} , CHRIS P. DUIF³ , WIM G. BOUWMAN³ , ROGER PYNNE^{1,4,5,6} , ROBERT M. DALGLIESH² , AND FANKANG LI¹ 

¹Neutron Technologies Division, Oak Ridge National Laboratory, Oak Ridge, TN, USA

²ISIS Neutron and Muon Source, Science and Technology Facilities Council, Rutherford Appleton Laboratory, Didcot, United Kingdom

³Faculty of Applied Sciences, Delft University of Technology, Delft, The Netherlands

⁴Department of Physics, Indiana University, Bloomington, IN, USA

⁵Center for Exploration of Energy and Matter, Indiana University, Bloomington, IN, USA

⁶Quantum Science and Engineering Center, Indiana University, Bloomington, IN, USA


Spin-echo small-angle neutron scattering (SESANS) is a unique method to measure structures of materials in real space with length scales from $\sim 30 \mu\text{m}$ to $\sim 20 \mu\text{m}$ [1]. As shown in Figure 1, the accessible length scale of SESANS is given by its ability to encode the momentum transfer into the Larmor phase, namely $\Phi = \vec{\delta} \cdot \vec{Q}$, where \vec{Q} is the momentum transfer and $\vec{\delta}$ is the encoding vector of the setup and its projection along Q (δ_Q) is called spin-echo length (SEL). The spin echo length, which is synonymous with the spatial correlation distance probed, is defined as the following [2]

$$\delta_Q \propto \lambda^2 BL \cot \theta \quad (1)$$

where λ is neutron wavelength, B is magnetic field, L is length of the parallelogram magnetic field region, and θ is the angle between the inclined magnetic field boundary and the beam direction, as shown in Figure 1. The result of the SESANS experiment is a Hankel transformation of the SANS scattering function $I(Q)$, which yields the correlation function of the sample in real space [29].

Various approaches have been deployed to implement SESANS around the world, including radio-frequency (RF) neutron spin flippers (Offspec, Larmor at the ISIS Neutron and Muon Source [3,4]), tilted Permalloy films (TU Delft Reactor Institute Delft [5]), and magnetic Wollaston prisms (MWP) (SESAME of Indiana University Low Energy

Neutron Source, LENS [6] and Oak Ridge National Laboratory High Flux Isotope Reactor, ORNL HFIR [7]). Figure 2 shows the photos of SESANS instruments at ISIS (Larmor), TU Delft, and ORNL. Both the Offspec and Larmor instruments at ISIS utilize four adiabatic fast passage (AFP) RF flippers, and the SEL can be scanned in λ using time-of-flight (TOF) for a given θ , defined as the angles of the static field magnets inside the RF flipper relative to the beam direction (the pole shoe angle). In a single measurement, the magnetic field strength B is fixed, but there are multiple configurations that allow for different field strengths, which can be varied when required. The SESANS instrument at TU Delft utilizes four magnetized Permalloy foils with each foil optimized as π flippers for a neutron wavelength of $2.10(5) \text{ \AA}$. The tilt angle of these foils is 5.5° relative to the beam and the SEL is scanned by changing the magnetic field B . While there is no permanent and fully optimized SESANS instrument at ORNL, its capability has been demonstrated at HB-2D polarized test beamline of the High Flux Isotope Reactor (HFIR) [8] with MWPs [9] at a neutron wavelength of $4.25(2) \text{ \AA}$. The superconducting MWPs offer advantages including high spin transport efficiency, minimal neutron attenuation, and reduced parasitic scattering. The SEL is scanned by changing the magnetic field. The different instruments, therefore, vary the SEL using different components of Equation (1): the magnetic field B at ORNL and TU Delft and the wavelength λ and angle between the field and beam θ at Larmor.

 Supplemental data for this article can be accessed online at <https://doi.org/10.1080/10448632.2025.2468088>.

© 2025 The Author(s). Published with license by Taylor & Francis Group, LLC

This is an Open Access article distributed under the terms of the Creative Commons Attribution-NonCommercial-NoDerivatives License (<http://creativecommons.org/licenses/by-nc-nd/4.0/>), which permits non-commercial re-use, distribution, and reproduction in any medium, provided the original work is properly cited, and is not altered, transformed, or built upon in any way. The terms on which this article has been published allow the posting of the Accepted Manuscript in a repository by the author(s) or with their consent.

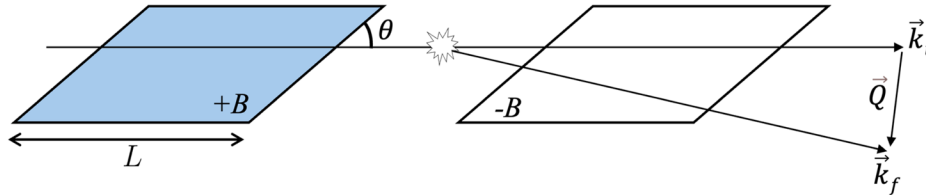


Figure 1. The schematic of a conventional SESANS setup composed of two parallelogram shaped regions of magnetic field of equal strength (B) in opposite directions. The momentum transfer (Q) is encoded into the Larmor phase of neutron spin.

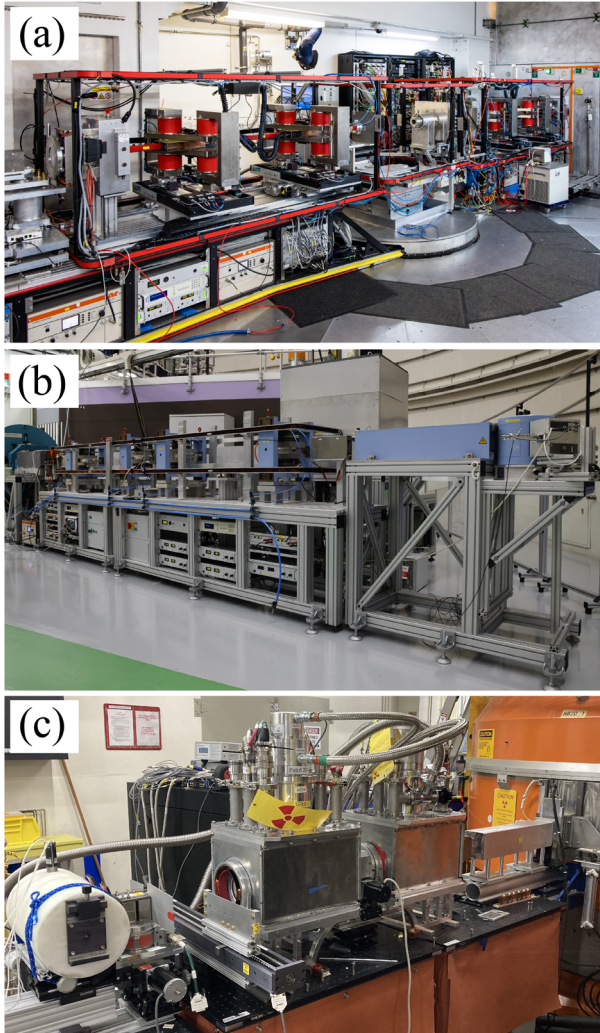


Figure 2. Photos of the SESANS instruments at (a) ISIS (Larmor) © STFC, (b) TU Delft, and (c) ORNL.

To ensure instrument reproducibility and independence of neutron wavelength and sample thickness, the normalized scattering correlation function $\ln(P/P_0)/(\lambda^2 t)$ is used as a consistent metric across the different techniques and devices, where P and P_0 are the spin-echo po-

larizations of the sample and blank and t is the sample thickness. This normalizes for all the instrument and sample variables that can impact measurements (λ and t), giving a truly instrument-independent parameter. The nomenclature and units for SESANS data are suggested by the SESANS Reproducibility Working Group [10].

The SESANS instruments at ISIS, TU Delft and ORNL have previously demonstrated the ability to perform SESANS measurements. Each instrument calibrates the SEL independently, using a variety of standard samples such as optical gratings [11, 12], aluminum wires [13], or quartz wedges [7, 14] with respect to various techniques, including SAXS [15], USANS [16], and SEMSANS [7]. In a recent example, the SESANS instruments at ISIS and ORNL were employed to measure the same colloidal sample [17], which gave a preliminary indication that the same samples, measured on different instruments, could give comparable data. To compare and benchmark the performance of the world's currently operational instruments, we have designed a cross-calibration study, choosing two solid inorganic samples that are stable and consistent with time to ensure reproducibility and reliability across these SESANS instruments. In the following discussion, we will present the results obtained using the SESANS instruments from ISIS, TU Delft, and ORNL representing different types of approaches.

Round-robin measurements were conducted on two samples: a nanoporous alumina membrane [18] and a flexible graphite sheet [19]. The exact same samples were measured at these three facilities. The alumina membrane comprises round cylindrical pores with a mean pore radius of 50 nm and a pore length of 60 μm , which corresponds to the thickness of the film. Due to the regular distribution of the cylindrical pores, a strong correlation signal is expected. With a well-defined microstructure and stability, it is ideal for cross calibration of all these SESANS instruments. Additionally, the graphite sheet with a thickness of 0.45 mm was measured. It is composed entirely of solid graphite and void spaces and exhibits power-law scattering in the SANS region [20].

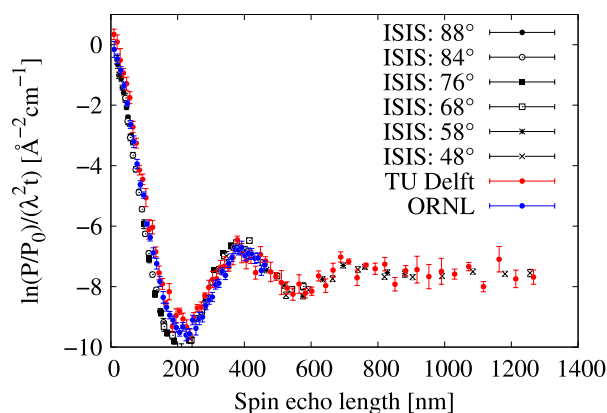


Figure 3. Normalized scattering correlation functions of the same nanoporous alumina membrane measured at SESANS instruments in ISIS, ORNL, and TU Delft. The listed angles are the poleshoe angles of RF flippers at Larmor. The RF flippers were operated at a frequency of 1 MHz.

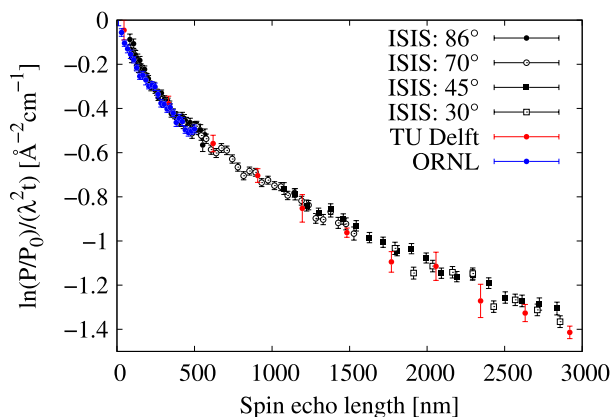


Figure 4. Normalized scattering correlation functions of the same flexible graphite sheet measured at SESANS instruments in ISIS, ORNL, and TU Delft. The listed angles are the poleshoe angles of RF flippers at Larmor. The RF flippers were operated at a frequency of

Owing to its high scattering intensity and the ability to adjust thickness by stacking sheets, the graphite sheet is ideal for successfully obtaining SESANS data, independent of the neutron flux available at each instrument.

Figures 3 and 4 show the results of this round-robin study. Figure 3 displays SESANS data of the same nanoporous alumina membrane taken among at these three facilities. For the ISIS data, several poleshoe angles θ were measured to vary the measurable SEL range in addition to the TOF method. They are also corrected for the amount of scattering lost between the transmission monitor and the main detector [21]. The Larmor data were measured with 21 poleshoe angles in total, and only selected results are shown [22]. The complete results can

be found in Figure S1. The oscillation of the correction function denotes the inter-correlations of the pores. The first dip and peak positions of $\ln(P/P_0)/(\lambda^2 t)$ are observed at ~ 200 and 400 nm in SELs for all results. The three experimental results agree well, which indicates that SELs of the three SESANS instruments are well calibrated. Figure 4 shows the normalized scattering correlation function obtained with the flexible graphite sheet. The Larmor data were measured with 7 poleshoe angles in total, and only selected results are shown [23]. The complete results can be found in Figure S2. A monotonic decay of the normalized scattering correlation function as SEL increases were observed, which is expected from the power-law scattering from the voids [24]. There is very good agreement between the experimental results, which demonstrates that all three SESANS instruments are well calibrated in their ability to accurately measure the absolute value of the normalized scattering correlation functions.

By measuring multiple samples that contain features at different length scales and with different degrees of total scattering, we have been able to investigate the reproducibility of multiple SESANS instruments. The agreement among all the instruments confirms the reliability the SESANS technique, the ability of each operational SESANS instrument to obtain the accurate SEL and normalized scattering correlation function, and confirms the data reproducibility between different SESANS instruments. Whatever SESANS instrument and approach to encoding polarization is chosen, we show that it is possible to obtain reproducible and reliable data.

Acknowledgments

This work was supported by the US Department of Energy (DOE), Office of Science, Office of Basic Energy Sciences, Early Career Research Program Award (KC0402010), under Contract No. DE-AC05-00OR22725. This research used resources at the High Flux Isotope Reactor, a DOE Office of Science User Facility operated by the Oak Ridge National Laboratory. We acknowledge ISIS Neutron and Muon Source for beamtime on Larmor. This manuscript was authored by UT-Battelle, LLC under Contract No. DE-AC05-00OR22725 with the U.S. Department of Energy. The United States Government retains and the publisher, by accepting the article for publication, acknowledges that the United States Government retains a non-exclusive, paidup, irrevocable, world-wide license to publish or reproduce the published form of this manuscript,

or allow others to do so, for United States Government purposes. The Department of Energy will provide public access to these results of federally sponsored research in accordance with the DOE Public Access Plan (<http://energy.gov/downloads/doepublicaccess-plan>). For the purpose of open access, the author has applied a Creative Commons Attribution (CC BY) licence to any Author Accepted Manuscript version arising.

Data availability statement

Measurement data from Larmor beamtime will be available after embargo at doi:10.5286/ISIS.E.RB2330507-1 and doi:10.5286/ISIS.E.RB2390094-1. Processed data from Larmor, TU Delft and ORNL are available from the Data Community of canSAS SESANS Reproducibility Working Group [25–28].

ORCID

Fumiaki Funama  <http://orcid.org/0000-0003-3280-8103>

Gregory N. Smith  <http://orcid.org/0000-0002-0074-5657>

Steven R. Parnell  <http://orcid.org/0000-0002-7044-6257>

Chris P. Duif  <http://orcid.org/0000-0002-3263-963X>
Wim G. Bouwman  <http://orcid.org/0000-0002-5331-8085>

Roger Pynn  <http://orcid.org/0000-0002-0867-7505>
Robert M. Dalgliesh  <http://orcid.org/0000-0002-6814-679X>

Fankang Li  <http://orcid.org/0000-0001-8859-0102>

References

- W. G. Bouwman, *Food Struct.* **30**, 100235 (2021). doi: [10.1016/j.foostr.2021.100235](https://doi.org/10.1016/j.foostr.2021.100235)
- M. Theo Rekveldt, *Nucl. Instrum. Methods Phys. Res. Sect. B.* **114** (3–4), 336 (1996). doi: [10.1016/0168-583X\(96\)00213-3](https://doi.org/10.1016/0168-583X(96)00213-3)
- Larmor Technical Information*, <https://www.isis.stfc.ac.uk/Pages/Larmor-Technical-Information.aspx> (accessed 12 Jul. 2024).
- J. Plomp, Doctor of Philosophy, Delft University of Technology, 2009.
- M. T. Rekveldt *et al.*, *Rev. Sci. Instrum.* **76** (3), 033901 (2005). doi: [10.1063/1.1858579](https://doi.org/10.1063/1.1858579).
- S. R. Parnell *et al.*, *Rev. Sci. Instrum.* **86**, 023902 (2015). doi: [10.1063/1.4909544](https://doi.org/10.1063/1.4909544).
- F. Funama *et al.*, *Rev. Sci. Instrum.* **95** (7), 073709 (2024). doi: [10.1063/5.0217884](https://doi.org/10.1063/5.0217884).
- L. Crow *et al.*, *J. Phys: Conf. Ser.* **746**, 012010 (2016). doi: [10.1088/1742-6596/746/1/012010](https://doi.org/10.1088/1742-6596/746/1/012010)
- F. Li *et al.*, *Rev. Sci. Instrum.* **85** (5), 053303 (2014). doi: [10.1063/1.4875984](https://doi.org/10.1063/1.4875984)
- SESANS Reproducibility Working Group, https://wiki.cansas.org/index.php/SESANS_Reproducibility_Working_Group (accessed 23 Oct. 2024).
- S. McKay *et al.*, *Phys. Rev. A.* **109**, 042420 (2024). doi: [10.1103/PhysRevA.109.042420](https://doi.org/10.1103/PhysRevA.109.042420).
- M. Trinker *et al.*, *Nucl. Instrum. Methods Phys. Res. Sect. A.* **579**, 1081 (2007). doi: [10.1016/j.nima.2007.06.008](https://doi.org/10.1016/j.nima.2007.06.008).
- J. Plomp *et al.*, *Nucl. Instrum. Methods Phys. Res. Sect. A.* **574**, 324 (2007). doi: [10.1016/j.nima.2007.02.068](https://doi.org/10.1016/j.nima.2007.02.068).
- M. Theo Rekveldt *et al.*, *Physica B Condens. Matter.* **350** (1–3), E791 (2004).
- K. van Gruijthuijsen *et al.*, *EPL.* **106** (2), 28002 (2014). doi: [10.1209/0295-5075/106/28002](https://doi.org/10.1209/0295-5075/106/28002)
- C. Rehm *et al.*, *Appl. Cryst.* **64**, 354 (2013). doi: [10.1107/S0021889812050029](https://doi.org/10.1107/S0021889812050029).
- C. M. Wolf *et al.*, *J. Appl. Cryst.* **57**, 1841 (2024). doi: [10.1107/S1600576724009944](https://doi.org/10.1107/S1600576724009944).
- SmartMembranes*, <http://www.smartmembranes.de/en/products/nanoporous-alumina/>, accessed: 2024-03-21.
- PAPYEX® Flexible Graphite*, <https://www.mersen.com/sites/default/files/publications-media/6-gs-papyex-graphite-souple-mersen.pdf> (accessed 9 May 2024).
- E. P. Gilbert *et al.*, *Faraday Trans.* **94** (13), 1861 (1998). doi: [10.1039/A801303I](https://doi.org/10.1039/A801303I)
- F. Li *et al.*, *Sci. Rep.* **9** (1), 8563 (2019). doi: [10.1038/s41598-019-44493-9](https://doi.org/10.1038/s41598-019-44493-9)
- G. N. Smith, *STFC ISIS Neutron Muon Source*. (2023). <https://doi.org/10.5286/ISIS.E.RB2390094-1>.
- G. N. Smith, *STFC ISIS Neutron Muon Source*. (2023). <https://doi.org/10.5286/ISIS.E.RB2330507-1>.
- R. Andersson *et al.*, *J. Appl. Cryst.* **41**, 868 (2008). doi: [10.1107/S0021889808026770](https://doi.org/10.1107/S0021889808026770).
- G. N. Smith. (2024). *Larmor SESANS Data of Papyex Flexible Graphite [Data set]*, Zenodo, [10.5281/zenodo.14066951](https://zenodo.org/record/14066951)
- G. N. Smith. (2024). *Larmor SESANS Data of FlexiPor Nanoporous Alumina [Data set]*, Zenodo, [10.5281/zenodo.14066678](https://zenodo.org/record/14066678)
- S. R. Parnell *et al.*, (2024). *TU Delft SESANS Data of Reproducibility Samples [Data set]*, Zenodo, [10.5281/zenodo.14161931](https://zenodo.org/record/14161931)
- F. Li *et al.*, (2024). *ORNL SESANS Data of Reproducibility Samples [Data set]*, Zenodo, [10.5281/zenodo.14161883](https://zenodo.org/record/14161883)
- W. G. Bouwman *et al.*, *Nucl. Instrum. Methods Phys. Res. Sect. A.* **529** (1–3), 16 (2004). doi: [10.1016/j.nima.2004.04.150](https://doi.org/10.1016/j.nima.2004.04.150)